

1 Shear rate effect on the residual strength characteristics of saturated loess in naturally  
2 drained ring shear tests

3

4 Baoqin Lian<sup>a,b</sup>, Xingang Wang<sup>a\*</sup>, Jianbing Peng<sup>b\*</sup>, Qiangbing Huang<sup>b</sup>

5

6 <sup>a</sup>State Key Laboratory of Continental Dynamics, Department of Geology, Northwest  
7 University, Xi'an 710069, China

8

9 <sup>b</sup>College of Geological Engineering and Surveying, Chang'an University, Key  
10 Laboratory of Western China Mineral Resources and Geological Engineering, Xi'an  
11 710054, China

12

13

14 \*Corresponding author

15

16

17

18

19 **Abstract**

20 Residual shear strength of soils is an important soil parameter for assessing the  
21 stability of landslides. To investigate the effect of the shear rate on the residual shear  
22 strength of loessic soils, a series of naturally drained ring shear tests were carried out  
23 on loess from three landslides at two shear rates (0.1 mm/min and 1 mm/min).  
24 Experimental results showed that the shear displacement to achieve the residual stage  
25 for specimens with higher shear rate was greater than that of the lower rate; both the  
26 peak and residual friction coefficient became smaller with increase of shear rate for  
27 each sample; at two shear rates, the residual friction coefficients for all specimens  
28 under the lower normal stress were greater than that under the higher normal stress.  
29 Moreover, specimens with almost the same low fraction of clay (CF) showed similar  
30 shear rate effect on the residual friction coefficient with normal stress increasing,  
31 whereas specimen with high CF (24%) showed the contrast tendency, indicating that  
32 such effect is closely associated with CF. The tests results revealed that the difference  
33 in the residual friction angle  $\phi_r$  at the two shear rates,  $\phi_r(1) - \phi_r(0.1)$ , under each  
34 normal stress level were either positive or negative values of which the maximum  
35 magnitude is about  $0.8^\circ$ . However, the difference  $\phi_r(1) - \phi_r(0.1)$  determined under all  
36 normal stress levels was negative, which indicates that the residual shear parameters  
37 reduced with the increasing of the shear rate in loess area. Such negative shear rate  
38 effect on loess could be attributed to a greater ability of clay particles in specimen to  
39 restore broken bonds at low shear rates.

40 **Keywords:** Loess; Residual shear strength; Ring shear test; Shear rate; Residual shear  
41 parameter

42

## 43 **1. Introduction**

44 Residual shear strength of soil is of great significance for evaluating the stability  
45 for the slip surface of first-time landslides as well as reactivated landslides (Bishop et  
46 al., 1971; Mesri and Shahien, 2003; Tiwari and Latha, 2019; Li et al., 2017). The  
47 residual strength of soils is defined as the minimum constant value of strength along  
48 the slip plane, in which the soil particles are reoriented and subjected to sufficiently  
49 large displacements in relatively low shear rate (Skempton, 1985).

50 Numerical studies have been done to assess the residual strength through the  
51 laboratory tests using ring shear tests and reversal direct shear tests (Vithana et al.,  
52 2012; Summa et al., 2018; Moeyersons et al., 2008; Chen and Liu, 2013; Summa et al.,  
53 2010). It is a generally accepted fact that the measurement of the residual strength is  
54 most preferred done with a ring shear test since it allows the soil specimen be sheared  
55 at unlimited displacement which can simulate the field conditions more accurately  
56 (Sassa et al., 2004; Tiwari and Marui, 2005; Lupini et al., 1981; Bhat, 2013). Until now,  
57 great efforts have been paid to the study of the shear rate effect on the minimum value  
58 of clay or sand strength at residual states (Li et al., 2017; Tika and Hutchinson,  
59 1999; Suzuki et al., 2007; Grelle and Guadagno, 2010; Lemos, 1985; Tika,  
60 1999; Morgenstern and Hungr, 1984). As a result, the residual strength of clay or sand  
61 under the effect of shear rate has been made relatively clear. However, compared with  
62 the results of tests on clay or sand, understanding of the shear characteristics of silty  
63 soil, such as loess, is not yet complete. As pointed out by Ding (2016), some drained  
64 ring shear tests have concluded that the increase in shear rate causes the residual

65 strength of loess to increase. On the contrary, Kimura et al. (2014) reported that the  
66 residual strength of Malan loess decreases with the increase of shear rate. Furthermore,  
67 Wang et al. (2015) found that the effect of shear rate on residual strength of loess is  
68 closely associated with the normal stress levels, and the change in residual strength of  
69 loess samples under high normal stress levels is small in ring shear tests.

70 Therefore, some inconsistent or even opposite results have been reported in the  
71 ring shear tests on loess above, which maybe attributed to the differences in the grain  
72 size distribution and mineral composition of the different material tested in previous  
73 studies (Ajmera et al., 2012). Particularly, this discrepancy maybe due to the  
74 difference in quantity and mineralogy of clay fraction (Nakamura et al., 2010;Li et al.,  
75 2013). Therefore, the previous studies on the effect of shear rate on residual strength  
76 of loess implied that there is still a lack of experimental data on this topic. From the  
77 above investigations, it can be concluded that the effect of the shear rate on the  
78 residual strength of the loess is not fully understood and needs further scrutiny.  
79 Moreover, it should be noted that the residual strength parameters (friction angle)  
80 obtained from using different shear rates may be adopted to provide a guide for  
81 designing some precision engineering which require high accuracy of the design  
82 parameters, thus, the effect of the shear rate on the residual strength of soils should be  
83 fully investigated to determine the parameters with high reliability. In addition,  
84 residual strength parameters of soil play a key role in assessing the stability analysis  
85 of landslides (Xu et al., 2018;Wesley, 2018). Therefore, accurate determination of the  
86 residual strength parameters and their dependence on the shear rate may affect the

87 stability evaluation of landslides. Thus, it is necessary to study the change of residual  
88 strength of loess with shear rate in order to have a good understanding of the suitable  
89 approach for the residual strength parameters measurement.

90 In this backdrop, to clarify the residual shear characteristics of loess under the  
91 effect of the shear rate, a series of naturally drained ring shear tests were conducted on  
92 loess obtained from three landslides on the Loess Plateau in China at two shear rates  
93 (0.1 mm/min and 1 mm/min). The residual shear characteristics of loess at the  
94 residual state was examined. Considering that shear strength of loess reduces with  
95 moisture content (Picarelli, 2010;Zhang et al., 2009;Dijkstra et al., 1994), ring shear  
96 tests were conducted on saturated loess samples corresponding to the worst condition  
97 in field engineering. Furthermore, this study investigated the change in the residual  
98 strength parameters of loess at different shear rates and the relationship between the  
99 residual strength parameters with the normal stress in naturally drained ring shear  
100 tests as well.

101

## 102 **2. Geological setting of landslide sites**

103 Soil samples from three landslides in the northwest of China were selected in this  
104 study. Soil samples used for the ring shear tests and index measuring tests  
105 predominantly consist of loess deposits and were collected in a disturbed condition.  
106 For convenience, the names of landslide sites were abbreviated into Djg, Ydg and  
107 Dbz. Fig. 1 shows the study sites and some views of the landslides.

### 108 **Dingjiagou landslide (Djg)**

109 The Djg landslide, located at the mouth of Dingjia Gully in Yan'an of China, is

110 geologically composed of upper loess and lower sand shale in the Triassic Yanchang  
111 formation (She, 2015). The dustpan-shaped landslide is inclined to the east, with its  
112 inclination  $75.85^\circ$ . The landslide is 350 m in width, 180 m in length, 70 m in elevation.  
113 The average thickness of slip mass is around 20 m, and the volume of landslide  
114 totaled approximately  $105 \times 10^4 \text{ m}^3$ . The slip mass is mainly constituted by loess,  
115 whereas the sliding bed consists of sand shale in Yan-chang formation. The thickness  
116 of the sliding zone varied from 30 to 50 cm. The front lateral region of the main slide  
117 section of the Djg landslide, where the sampling was performed, was found to be silty  
118 clay.

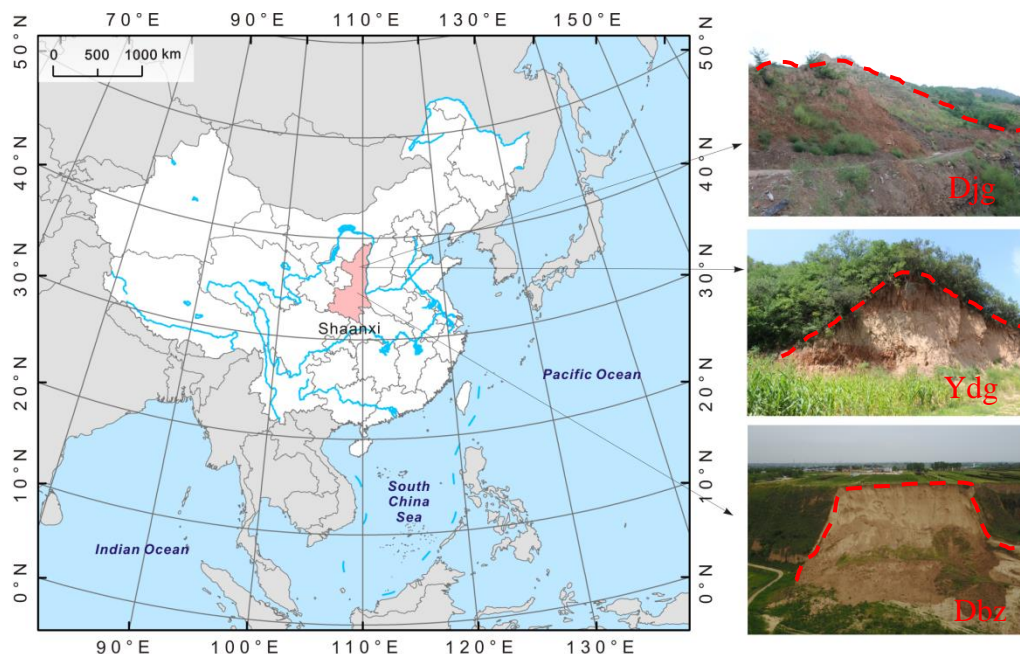
#### 119 **Yandonggou landslide (Ydg)**

120 The Ydg landslide, located in the Qiaogou town of Yan'an in Shaan xi province of  
121 China. The top and the toe altitude of the landslide are about 1165 m and 1110 m  
122 above the sea level, with the height difference between the toe and the top of landslide  
123 about 55 m. The slides have well-developed boundaries with the main sliding  
124 direction of  $240^\circ$  and slope angle of  $30^\circ$ . From the landslides profile, the sliding masses  
125 from top to bottom were classified by late Pleistocene ( $Q_3$ ) loess, Lishi ( $Q_2$ ) loess and  
126 clay soil, respectively (Zhang et al., 2006). Multiple landslides had occurred in this  
127 site, and the soil samples used in this study were collected from  $Q_2$  loess stratum  
128 within the slide ranged from 4.5 m to 18 m in height.

#### 129 **Dabuzi landslide (Dbz)**

130 The Dbz landslide located in the middle part of Shaanxi province (about E  
131  $108^\circ 51' 36''$  and N  $34^\circ 28' 48''$ ), China, which is a semi-arid zone dominated by loessic  
132 geology (Yan et al., 2015). In this region, the investigated site is classified as a typical

133 loess tableland with Quaternary stratum (Ma et al., 2019). The sedimentary losses in  
134 this area are grey yellow, and the exposure stratum in this area has been divided into  
135 two stratigraphic units, namely, the upper Malan (Q<sub>3</sub>) loess and the lower Lishi (Q<sub>2</sub>)  
136 loess, of which the Q<sub>3</sub> loess is younger. The Q<sub>3</sub> loess is closest to the surface and is up  
137 to approximately 12 m thick, while the thickness of Q<sub>2</sub> loess may reach an upper limit  
138 of about 50 m (Leng et al., 2018). The loess in this area have well-developed vertical  
139 joints (Sun et al., 2009). The travel distance and the maximum width of the slip mass  
140 are roughly estimated to be 122 m and 133 m, respectively. The armchair-shaped  
141 landslide shows an apparent sliding plane, with an area of approximately 15,660 m<sup>2</sup>  
142 and about 66.25 m maximum difference in elevation. The main direction of this  
143 landslide is approximately 355°. The exposed side scarp of the landslide, where the  
144 sampling was done, was found to be entirely in the Q<sub>2</sub> loess stratum.



146 Fig. 1. Location of study sites and some views of landslides (after Hu et al., 2018)

147 Notes: Red dashed lines in the Fig. 1 represent landslide boundary.

### 148 3. Experimental scheme

149 **3.1. Testing sample**

150 The fact that the residual shear strength is independent of the stress history has  
151 been reported by many researchers (Bishop et al., 1971; Stark et al., 2005; Vithana et  
152 al., 2012). Thus, disturbed loess samples from each landslide weighing about 25 kg  
153 were collected to investigate the residual shear strength.

154 The soil samples were air-dried, and then crushed with a mortar and pestle as it  
155 has been reported that crushing samples were suitable to determine the residual  
156 strength of the remoulded soils (Stark et al., 2005). It was found that small lumps may  
157 exist in air-dried samples, which may be too big for the cell, so lumps were crushed in  
158 order to make sample uniform. This should be done with care so as not to destroy  
159 silty-dominated loess. After that, soil samples were processed through 0.5 mm sieve.  
160 Distilled water was then added to the soil samples until saturated water content were  
161 obtained. The physical parameters such as natural moisture content (*in-situ* moisture  
162 content), specific gravity, bulk density, plastic limit, and liquid limit were determined  
163 in accordance with the Chinese National Standards (CNS) GB/T 50123-1999  
164 (standards for soil test methods) (SAC, 1999), but clay size was defined to be less  
165 than 2  $\mu\text{m}$  followed ASTM, D 422 (ASTM, 2007). Each soil sample was separated  
166 into clay (sub 0.002 mm), silt (0.002-0.075 mm), and sand (0.075-0.5 mm) fractions.  
167 The physical indexes of the soil are listed in Table 1.

168 The grain size distribution of soil was measured using a laser particle size  
169 analyzer Bettersize 2000 (Dandong Bettersize Instruments Corporation, Dandong,  
170 China). The sieved soil samples were used to determine particle size distribution. In



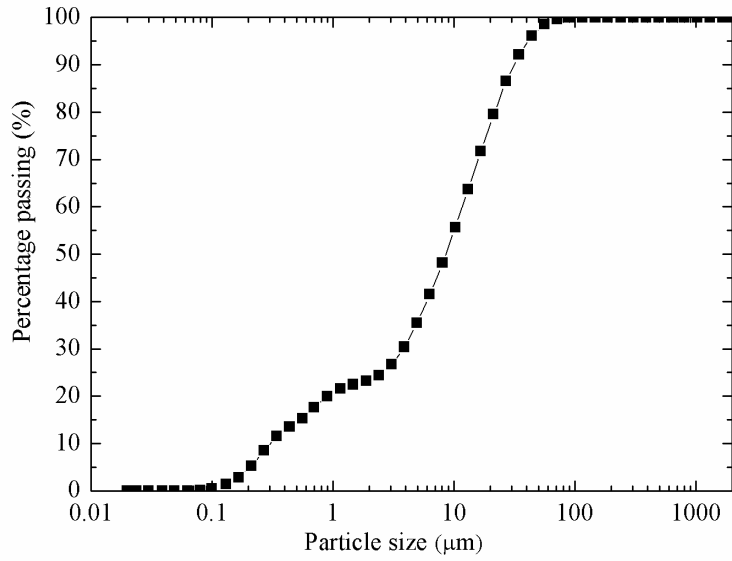
171 this study, soil samples were treated with sodium hexaphosphate, serving as a  
 172 dispersant, to disaggregate the bond between the particles. The particle size  
 173 distribution curves of soils were shown in Fig. 2. The results show that the clay  
 174 fraction in Djg landslide soil (24%) is more than two times than that from Ydg (9%)  
 175 and Dbz (9.1%). Furthermore, the particle size analysis illustrated that the percentage  
 176 of silt-sized soil in three landslides ranged from 75.66% to 87.4%. In addition, Ydg  
 177 landslide soil consists of the greatest percentage of the sand fraction which reaches up  
 178 to 10.55% (Table 2 and Fig. 2).

179  
 180  
 181  
 182

183 **Table 1.** Physical parameters of slip-zone loess.

| sites | $\rho_d$ | w    | $\rho$ | $G_s$ | $W_L$ | $W_p$ | Grain size fractions (%) |               |               |             |
|-------|----------|------|--------|-------|-------|-------|--------------------------|---------------|---------------|-------------|
|       |          |      |        |       |       |       | <0.002mm                 | 0.002-0.005mm | 0.005-0.075mm | 0.075-0.5mm |
| Djg   | 1.74     | 19.5 | 2.08   | 2.65  | 36    | 20    | 24                       | 11.48         | 64.18         | 0.34        |
| Ydg   | 1.47     | 18   | 1.74   | 2.71  | 33    | 19    | 9                        | 5.28          | 75.17         | 10.55       |
| Dbz   | 1.48     | 16   | 1.72   | 2.70  | 32    | 21    | 9.1                      | 6.4           | 81            | 3.5         |

184 Notes:  $\rho_d$ = dry density ( $\text{g}/\text{cm}^3$ ); w=moisture content (%);  $\rho$ = bulk density ( $\text{g}/\text{cm}^3$ );  $G_s$   
 185 = specific gravity;  $W_L$ =liquid limit (%);  $W_p$ = plastic limit (%).

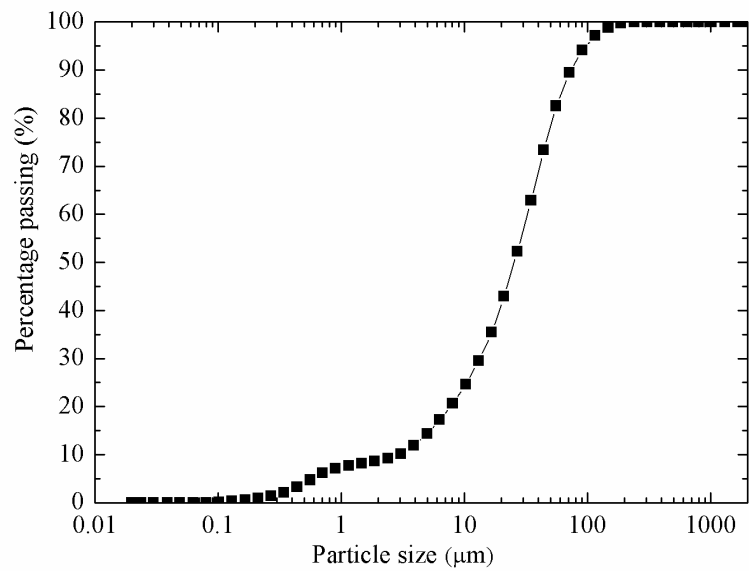


186

187

(a) Particle size distribution curve of soil obtained from DJG

188

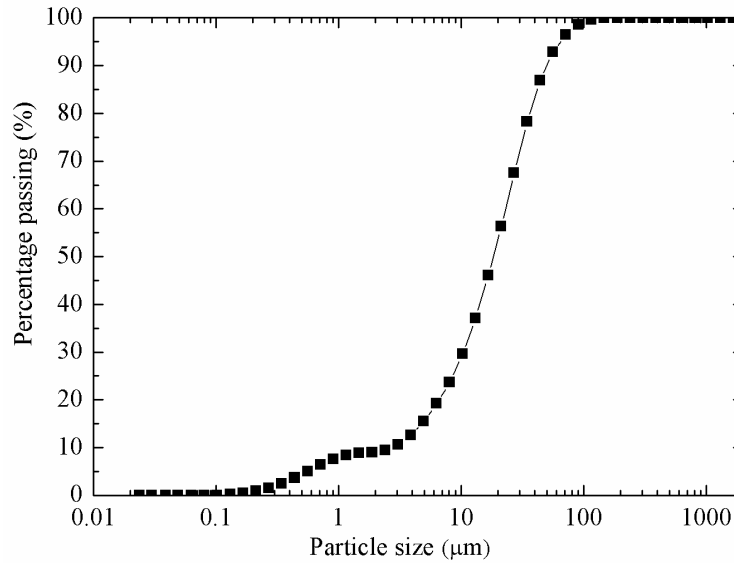


189

190

(b) Particle size distribution curve of soil obtained from YDG

191



192

(c) Particle size distribution curve of soil obtained from DBZ

193

194 Fig. 2. Particle size distribution curves.

195

### 196 3.2. Testing apparatus

197 An advanced ring shearing apparatus (SRS-150), the Bromhead-type ring shear

198 apparatus, manufactured by GCTS (Arizona, USA) was adopted in ring shear tests

199 and the photos of apparatus were shown in Fig. 3, which consists mainly of a shear

200 box with an outer diameter of 150 mm, an inter diameter of 100 mm and the maximal

201 sample height of 250 mm. The shearing box consists of the upper shear box and the

202 lower shear box. In the shearing process, the upper shear box keeps still while the

203 lower one rotates. The apparatus, which provides an effective specimen area of 98

204 cm<sup>2</sup>, is capable of shearing the specimen for large displacements. The annular

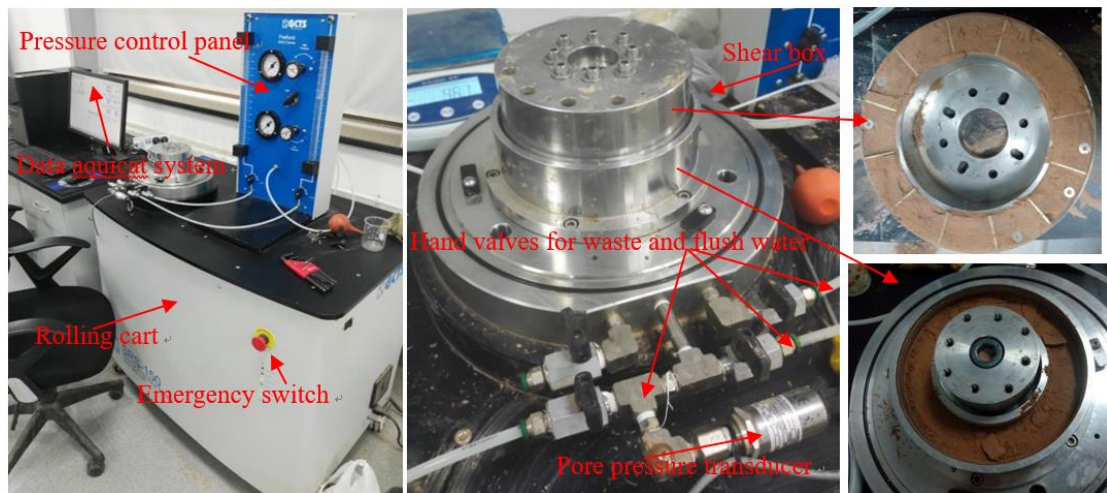
205 specimen is confined by inside and outside metal rings. Moreover, the specimen is

206 confined by bottom annular porous plates and top annular porous plates in which have

207 sharp-edged radial metal fins which protrude vertically into the top and bottom of the

208 specimen at the shearing process. Two annual porous plates were used to provide

209 drainage condition in the test following previous research (Stark and Vettel, 1992).  
210 The normal stress, shear strength and shear displacement can be monitored by  
211 computer in shearing process. The measurement features of the ring shear apparatus  
212 employed in this study are described as follows: shear rate range from 0.001 degrees  
213 to 360 degrees per minute, 10 kN axial load capacity, 300 Nm continuous torque  
214 capacity, maximum normal stress of 1000 kN/m<sup>2</sup>.  
215



216  
217 Fig. 3. Ring shear apparatus (SRS-150)

### 218 3.3. Testing procedure

219 This study was comprised of 3 groups of test results, in which 24 remolded  
220 saturated loess samples were sheared with normal stress ranging from 100 to 400  
221 kN/m<sup>2</sup> under two shear rates. In present study, reconstituted samples of the sub 0.5  
222 mm soil fractions were prepared for the shear tests as it was reported that the residual  
223 strength of the soil was unaffected by its initial structure (Vithana et al., 2012; Bishop  
224 et al., 1971). Consolidated drained (CD) tests with single-stage shear was performed.  
225 Here, the single-stage shear means shearing the sample under effective pressure or  
226 stress conditions after the consolidation of the sample. Specimens were first prepared

227 by adding distilled water to the air-dried soil until the saturated moisture contents  
228 were obtained. Then, specimens were kept in a sealed container for at least one week  
229 to fully hydrate. Afterwards, specimens are reconstituted in the ring-shaped chamber  
230 of the apparatus by compaction. During the compaction process, samples were  
231 divided into equal five parts and each part was poured into the shear box and  
232 compacted. Samples with a height of 2.5 cm in this study were prepared in five layers  
233 of equal height to achieve the required density. The specimen was then consolidated  
234 under a specific effective normal stress in a range of 100 kN/m<sup>2</sup> to 400 kN/m<sup>2</sup> until  
235 consolidation was achieved. In this study, consolidation was completed when the  
236 consolidation deformation was smaller than 0.01 mm within 24 hr (Kramer et al.,  
237 1999;Shinohara and Golman, 2002). In ring shear tests, the normal stress at the  
238 shearing was the same as at consolidation stage. Shear strength of loess specimen was  
239 recorded at intervals of 1s before the peak shear strength, after the peak, the sampling  
240 rate was increased to 1 min.

241 In this study, ring shear tests were performed in a single stage under naturally  
242 drained condition and the samples were subjected to shearing until the residual state  
243 was achieved. Following the Bromhead (1992), the residual state was defined when a  
244 constant shear stress is obtained for more than half an hour. Drained condition of the  
245 shearing process is provided by two porous stones attached on the top and the bottom  
246 platen of the specimen container. As for soil specimens with low permeability, the  
247 rate of excess pore pressure generation in the shear box may exceeded that of  
248 pore-pressure dissipation, this type of condition is identified as naturally drained

249 condition in previous studies (Okada et al., 2004). Furthermore, Tiwari (2000)  
250 asserted that it was acceptable to use a shear rate below 1.1 mm/min to simulate the  
251 field naturally drained condition. Thus, shear rates of 0.1 mm/min and 1 mm/min  
252 were used in this study to simulate the naturally drained condition of the slip zone  
253 soils.

#### 254 **4. Results and discussion**

255 Twenty-four specimens were tested to investigate the residual shear characteristics  
256 of the saturated loess in the ring shear apparatus. Residual shear strength of loess was  
257 determined following the research conducted by Bromhead (1992) who pointed out  
258 that the residual stage is attained if a constant shear stress is measured for more than  
259 half an hour. Tests results are shown in this section.

##### 260 **4.1. Shear behavior**

261 Figs. 4(a)-6(a) show the typical shear characteristics of the loess (shear rate of 0.1  
262 mm/min and 1 mm/min) obtained from three different locations, where, the shear  
263 stress is plotted against the shear displacement. It is a widely accepted fact that  
264 normal stress has effect on the shear behavior of the soil (Wang et al., 2019;Eid,  
265 2014;Kimura et al., 2015;Stark et al., 2005;Eid et al., 2019), thus, the shear behavior  
266 of samples at the peak and residual stages, where, the determined peak friction  
267 coefficient as well as residual friction coefficient are plotted in Figs. 4(b)-6(b) against  
268 the corresponding effective normal stresses as well. The friction coefficient is defined  
269 as the shear stress divided by the effective normal stress.

270 Figs. 4(a)-6(a) demonstrate that shear stress increases dramatically within small

271 shear displacement and then reduces with shear displacement, until residual  
272 conditions were achieved at large displacements. Furthermore, it is obvious that the  
273 peak strength and the residual strength of samples with high shear rate (shear rate  
274 equal to 1 mm/min) are almost smaller than that of the samples with low shear rate  
275 (shear rate equal to 0.1 mm/min). It can be found that shear displacement to achieve  
276 the residual stage for specimens with high shear rate is greater than that of the low  
277 rate. For example, the minimum shear displacements for attaining residual condition  
278 for Djg specimens with low and high shear rate were about 360 mm and 650 mm,  
279 respectively. Under the shear rate of 0.1 mm/min and 1 mm/min, Ydg specimens need  
280 approximately 80 mm and 1,400 mm displacement to achieve residual stage. However,  
281 Dbz specimens require about 40 mm and 60 mm displacement to reach residual  
282 condition for low and high shear rate, respectively.

283 In Figs. 4(a)-6(a), a clear drop can be seen, at any normal stress, for specimens  
284 obtained from all sites. During shearing, as reported by Terzaghi et al. (1996), strain  
285 softening exhibits a dilative behavior for soils. It is seen that the shear behavior is  
286 non-linear against the shear displacement. The loess in Djg, Ydg and Dbz exhibited  
287 the typical shear stress and shear strain relationship, i.e., the strain softening behavior  
288 for a given shear rate (Figs. 4(a)-6(a)). As seen in Figs. 4(a)-6(a), the lower shear rate  
289 results in a more obvious dilation effect during the shearing process with a specific  
290 normal stress. It is obvious that Djg specimens showed greater peak-post drop than  
291 that of Ydg and Dbz specimens. For example, at the normal stress of 100 kN/m<sup>2</sup>, Djg  
292 samples show approximately 47.3% and 36.8% decrease from the peak friction

293 coefficient to the residual friction coefficient at low and high shear rates (Fig. 4(b)),  
294 respectively, which is greater than in the Ydg samples (about 9.8% and 10.3% in Fig.  
295 5(b)) and Dbz samples (about 2.4% and 3.2% in Fig. 6(b)). In Djg samples, an  
296 obvious slickenside was observed on the shear surface (Fig. 7). This phenomenon  
297 indicates a high degree of reorientation of platy clay minerals parallel to the direction  
298 of shearing. In Figs. 4(b)-6(b), on average, it was found that the decrease in the  
299 friction coefficient from the peak strength in the Djg sample is almost 18.1% and  
300 21.3% for the sample consolidated at normal stress of 400 kN/m<sup>2</sup> under the low and  
301 high shear rate (Fig. 4(b)), while such reduction in friction coefficient in Ydg sample  
302 are only about 4.1% and 4.8% (Fig. 5(b)). Furthermore, under the low and high shear  
303 rate, the friction coefficient reduction in Dbz samples are only approximately 5.6%  
304 and 6.0% (Fig. 6(b)). Skempton (1985) reported that the strength of soils falls to the  
305 residual value in ring shear tests, owing to reorientation of platy clay minerals parallel  
306 to the direction of shearing. Based on the conclusion that the post-peak drop in  
307 strength of normally consolidated soil is only due to particle reorientation after the  
308 peak strength (Skempton, 1964; Mesri and Shahien, 2003; Habibbeygi and Nikraz,  
309 2018), the results demonstrated that the Djg landslide soil existed the greater particle  
310 reorientation compared with that of other two landslide soils.

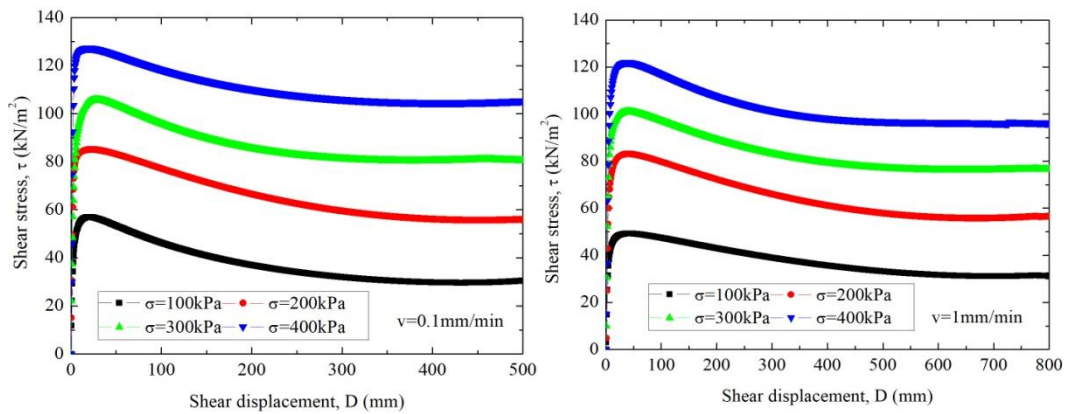
311

#### 312 **4.2. Effect of normal stress on the friction coefficients**

313 It can be seen from the Figs. 4(b)-6(b) that the friction coefficients (peak and  
314 residual) are higher at low effective normal stress levels (effective normal stress equal

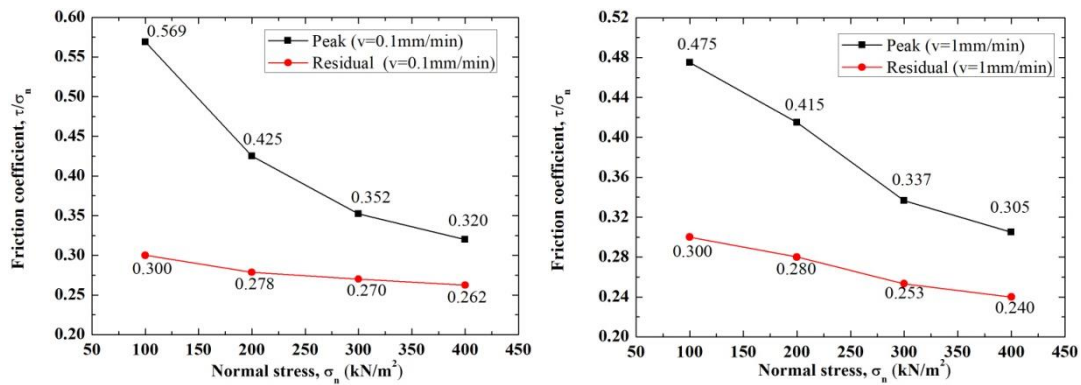


315 or less than  $100 \text{ kN/m}^2$ ) compared with that at high normal stress (effective normal  
 316 stress between 200 and  $400 \text{ kN/m}^2$ ). For example, with normal stress increasing from  
 317  $100 \text{ kN/m}^2$  to  $400 \text{ kN/m}^2$ , the peak and residual friction coefficient of Djg landslide  
 318 soils at the shear rate of  $0.1 \text{ mm/min}$  reduce from 0.569 to 0.32 and from 0.3 to 0.262  
 319 (Fig. 4(b)), respectively. Similarly, results obtained from other two landslides loess  
 320 also show that the friction coefficients decrease nonlinearly with normal stresses (Figs.  
 321 5(b) and 6(b)). Furthermore, specimens with shear rate of  $0.1 \text{ mm/min}$  attained greater  
 322 friction coefficients than that with shear rate of  $1 \text{ mm/min}$  (Figs. 4(b)-6(b)).



323

324 (a) Relationship between shear stress and shear displacement

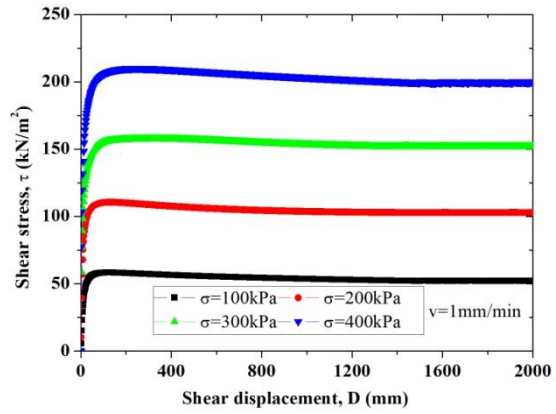
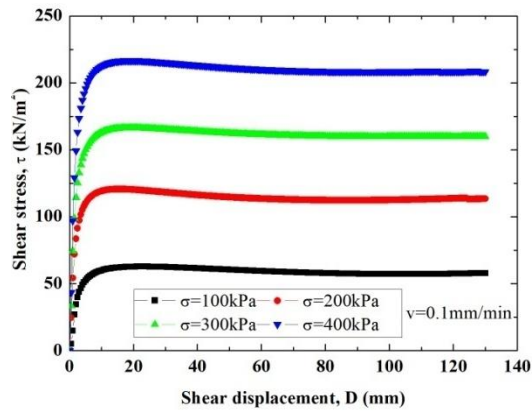


325

326 (b) Relationship between friction coefficient and normal stress

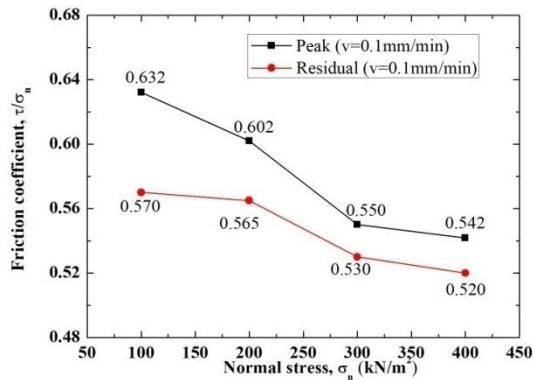
327 Fig. 4. Shear behavior characteristics of Djg soil samples

328

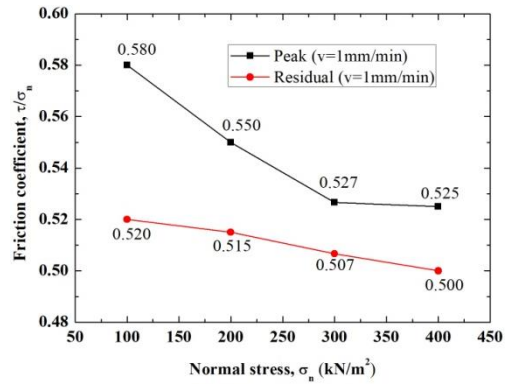


329

330 (a) Relationship between shear stress and shear displacement

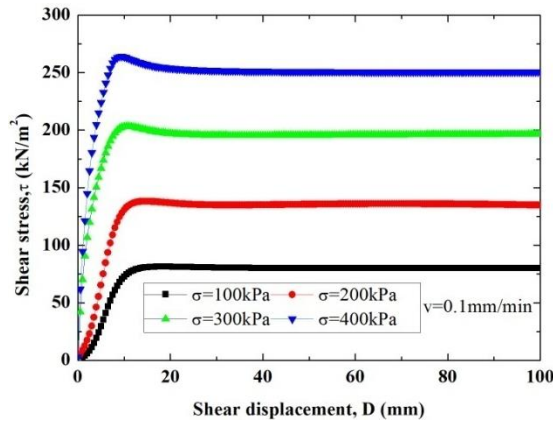


331

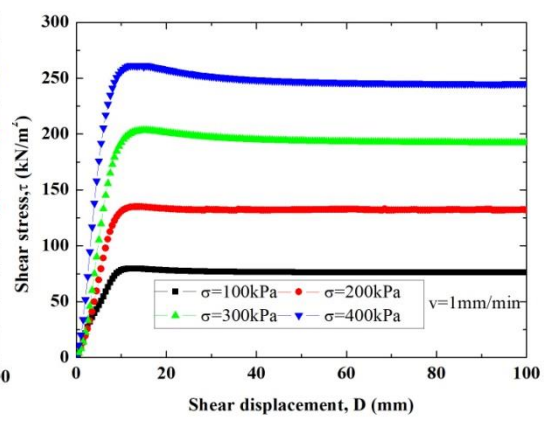


332 (b) Relationship between friction coefficient and normal stress

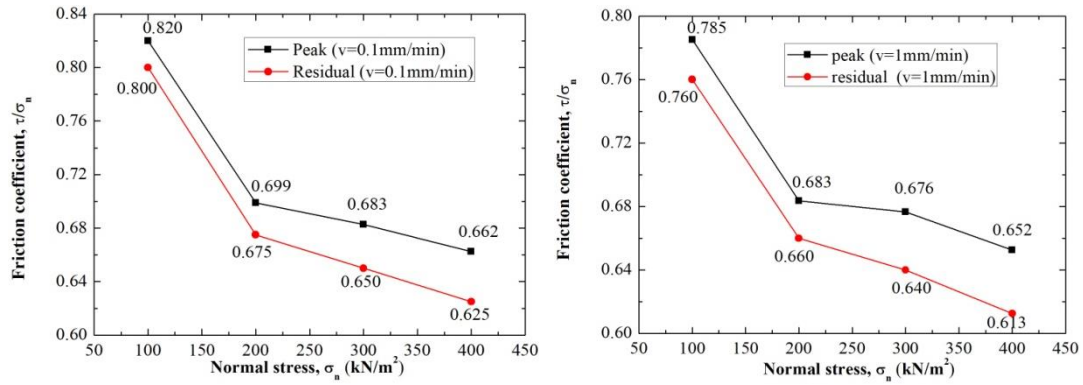
333 Fig. 5. Shear behavior characteristics of Ydg soil samples



334



335 (a) Relationship between shear stress and shear displacement



(b) Relationship between friction coefficient and normal stress

Fig. 6. Shear behavior characteristics of the Dbz soil samples

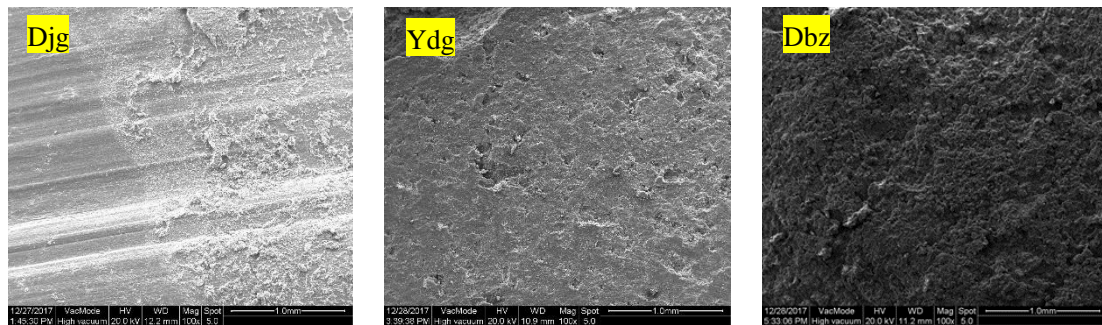


Fig. 7. SEM photographs of the shear surface of loess samples (100 magnification)

### 4.3. Effects of shear rate on residual strength parameter

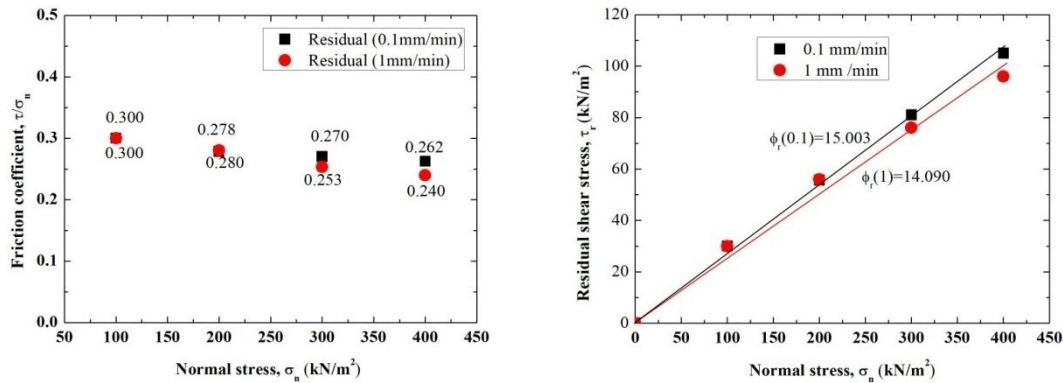
Following the previous study reported by (Eid et al., 2019; Terzaghi et al., 1996), the maximum value during shear process can be the peak shear stress, whereas the minimum value can be the minimum shear stress. Correspondingly, the maximum value can be referred to as the peak shear strength, whereas the minimum value can be referred to as the residual shear strength that resulted from particle rearrangements after a large shear displacement. Furthermore, the peak and residual strength parameters are determined by using Mohr–Coulomb failure criterion (Terzaghi et al., 1996). In this study, the residual strength parameters were analyzed and discussed.

For the samples described above, Figs. 8-10 show the relationships between the residual friction coefficient and the normal stress, and the residual strength parameters.

352 The residual friction coefficient is plotted against the normal stress. The residual  
353 friction coefficient is defined as the residual shear strength divided by normal stress. It  
354 has been recognized that the shear strength parameters including cohesion and friction  
355 angle (Terzaghi, 1951; Stark Timothy et al., 2005; Pakbaz et al., 2018). However,  
356 according to the previous studies, the residual angle of soils varies depended on the  
357 soil properties as well as the magnitude of normal stress provided the residual  
358 cohesion of soil is zero (Kimura et al., 2014; Skempton, 1964). Thus, in this study, the  
359 residual frictions are calculated by Coulomb's law assumed the residual cohesion is  
360 zero following the previous studies (Skempton, 1985). The residual strength  
361 parameters were defined as  $\phi_r(0.1)$  and  $\phi_r(1)$  at the low shear rate and high shear rate,  
362 respectively. And the difference between the residual friction angles at two shear rates  
363 was defined as  $\phi_r(1) - \phi_r(0.1)$ . Comparatively, the residual friction coefficient was  
364 defined as  $\tau_r/\sigma_n(0.1)$  at the low shear rate and  $\tau_r/\sigma_n(1)$  at the high shear rate,  
365 respectively. Furthermore, the difference between the residual friction coefficients  
366 was defined as  $\tau_r/\sigma_n(1) - \tau_r/\sigma_n(0.1)$ . Table 2 summarized the residual shear  
367 parameters of the landslide soils.

368 Fig. 8 shows that the residual friction coefficients are relatively low in Djg  
369 samples. The coefficients  $\tau_r/\sigma_n(0.1)$  and  $\tau_r/\sigma_n(1)$  at the normal stress of 100 kN/m<sup>2</sup>  
370 to 400 kN/m<sup>2</sup> ranged from 0.3 to 0.262 and from 0.3 to 0.24, respectively. The  
371 difference between the friction coefficients,  $\tau_r/\sigma_n(1) - \tau_r/\sigma_n(0.1)$ , at each normal  
372 stress level are varied in a range of -0.022 to +0.002. For the difference between the  
373 residual friction angles,  $\phi_r(1) - \phi_r(0.1)$ , ranged from -1.212° to +0.079° (Table 2). For

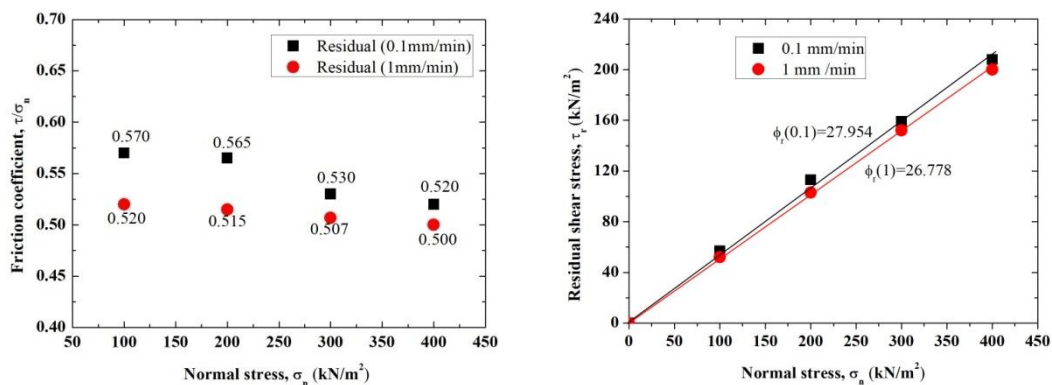
374 normal stress above 200 kN/m<sup>2</sup>, the residual friction coefficient  $\tau_r/\sigma_n(0.1)$  was found  
 375 to be greater than the residual friction coefficient  $\tau_r/\sigma_n(1)$ . For this sample, residual  
 376 friction coefficients show a slight decrease with the shear rate for normal stress above  
 377 200 kN/m<sup>2</sup>.



378

379 Fig. 8. Relationships between residual shear stress and normal stress, and residual  
 380 strength parameter for Djg soil sample

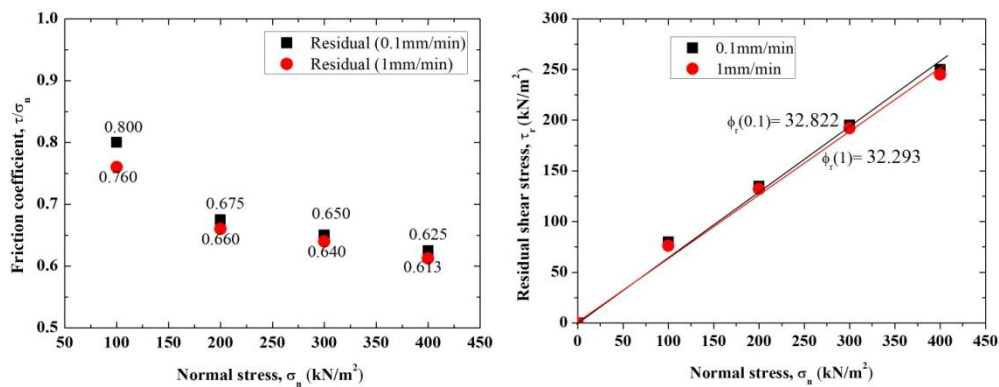
381 Fig. 9 gives the results of the Ydg samples. The coefficients  $\tau_r/\sigma_n(0.1)$  and  $\tau_r/\sigma_n$   
 382 (1) under the normal stress of 100 kN/m<sup>2</sup> to 400 kN/m<sup>2</sup> ranged from 0.57 to 0.52 and  
 383 from 0.52 to 0.50, respectively. Furthermore, the difference  $\tau_r/\sigma_n(1) - \tau_r/\sigma_n(0.1)$  at  
 384 each normal stress was from -0.05 to -0.02. As for the difference between the residual  
 385 friction angles,  $\phi_r(1) - \phi_r(0.1)$ , was in a range of -2.218° to -0.909°. In case of Ydg  
 386 soil sample, the residual friction coefficients decreased with increase of shear rate for  
 387 all normal stress levels.



388

389 Fig. 9. Relationships between residual shear stress and normal stress, and residual  
 390 strength parameter for Ydg soil samples

391 Fig. 10 presents the results of the Dbz samples. The coefficients  $\tau_r/\sigma_n(0.1)$  and  $\tau_r/\sigma_n(1)$   
 392  $\tau_r/\sigma_n(1)$  at the normal stress of 100 kN/m<sup>2</sup> to 400 kN/m<sup>2</sup> ranged from 0.8 to 0.625 and  
 393 from 0.76 to 0.613, respectively. The difference  $\tau_r/\sigma_n(1) - \tau_r/\sigma_n(0.1)$  at each normal  
 394 stress was from -0.04 to -0.01. The difference  $\phi_r(1) - \phi_r(0.1)$  was from -1.425° to  
 395 -0.405°. For Dbz samples, there was somewhat decrease tendency of the residual  
 396 friction coefficients with the increasing of the shear rate for all normal stress levels. It  
 397 is noted that the maximum difference was found at the lowest normal stress of 100  
 398 kN/m<sup>2</sup>.



399  
 400 Fig. 10. Relationships between residual shear stress and normal stress, and residual  
 401 strength parameter for Dbz soil sample

402 From the experimental results on the three selected landslides, it was found that  
 403 there is a negative relationship between residual friction coefficients and shear rates  
 404 for all samples (Figs. 8-10). Such a negative effect of shear rate (higher residual  
 405 friction coefficients at lower rates) has been reported in the literature for fine-grained  
 406 soils (Gratchev Ivan and Sassa, 2015;Tika et al., 1996). This effect may be closely  
 407 associated with ability of clay particles in specimen to restore broken bonds at

408 different shear rates. Previous scholars concluded that with higher shear rates, the  
409 breakdown of the bonds between clay particles or flocs exceeds the restoration bond,  
410 leading to reduction in residual friction coefficients (Osipov et al., 1984; Perret et al.,  
411 1996). In contrast, the bonds between particles are rebuilt quickly and the recovery  
412 rate can catch up the breakdown rate at lower shear rates. Therefore, the weaker  
413 bonding between particles could explain the strength drop with the increasing of the  
414 shear rate in this study.

415 As for Ydg and Dbz specimen, it is found that the shear rate effect on the friction  
416 coefficient can be seen to decrease with normal stress (Figs. 9-10). By contrast, there  
417 is an increasing tendency in the influence of shear rate on the friction coefficient with  
418 normal stress in Djg specimen (Fig. 8). Gibo et al. (1987) reported that the residual  
419 friction angle of soils was controlled by the effective normal stress as well as by the  
420 CF. Interestingly, Ydg (with CF 9%) and Dbz (with CF 9.1%) specimens with almost  
421 the same fraction of clay showed similar shear rate effect on the residual friction  
422 coefficient with normal stress increasing, however, Djg (with 24% CF) showed the  
423 contrast tendency of shear rate effect on residual friction coefficient with normal  
424 stress, indicating that such effect is closely associated with CF.

425 Table 2 summarizes residual strength parameters including  $\phi_r(0.1)$  and  $\phi_r(1)$  of  
426 all specimens obtained from the ring shear tests in this study. As for the Djg samples,  
427 the residual strength parameter  $\phi_r(0.1)$  and  $\phi_r(1)$  for all normal stress were found to  
428 be  $15.003^\circ$  and  $14.09^\circ$  (Fig. 8), respectively. However, the residual friction angles  $\phi_r$   
429 (0.1) and  $\phi_r(1)$  of the Ydg samples were obtained to be  $27.954^\circ$  and  $26.778^\circ$  (Fig. 9),

430 respectively. In the case of Dbz sample, the friction angles  $\phi_r(0.1)$  and  $\phi_r(1)$  were  
431 high,  $32.822^\circ$  and  $32.293^\circ$  (Fig. 10), respectively. The residual friction angles  $\phi_r(0.1)$   
432 and  $\phi_r(1)$  under all normal stresses were from  $15.003^\circ$  to  $32.822^\circ$  and from  $14.09^\circ$  to  
433  $32.293^\circ$ , respectively.

434 Due to the influence of the shear rate, the difference  $\phi_r(1) - \phi_r(0.1)$ , at each  
435 normal stress level varies in different locations, while the value of  $\phi_r(1) - \phi_r(0.1)$   
436 under all normal stress for the Djg, Ydg and Dbz samples were  $-0.913^\circ$ ,  $-1.176^\circ$  and  
437  $-0.529^\circ$ , respectively (Table 2). Wang (2014) and Fan et al. (2017) asserted that the  
438 residual shear strength of remolded loess hardly affected by shear rate below 5  
439 mm/min. However, the results in this study shown that  $\phi_r(1) - \phi_r(0.1)$  under all  
440 normal stress levels were negative for loess. Moreover, the absolute value of  $\phi_r(1) -$   
441  $\phi_r(0.1)$  in Ydg samples even reached up to  $1.176^\circ$ . Therefore, the ring shear test  
442 results provides a basis for some general comments on the use of tests results with  
443 different shear rates, partially deepening some aspects deriving from previous studies.

444

445

446

447

448

449

450

451

452

453

454



455 Table 2. Residual shear strength parameter of landslide soils.

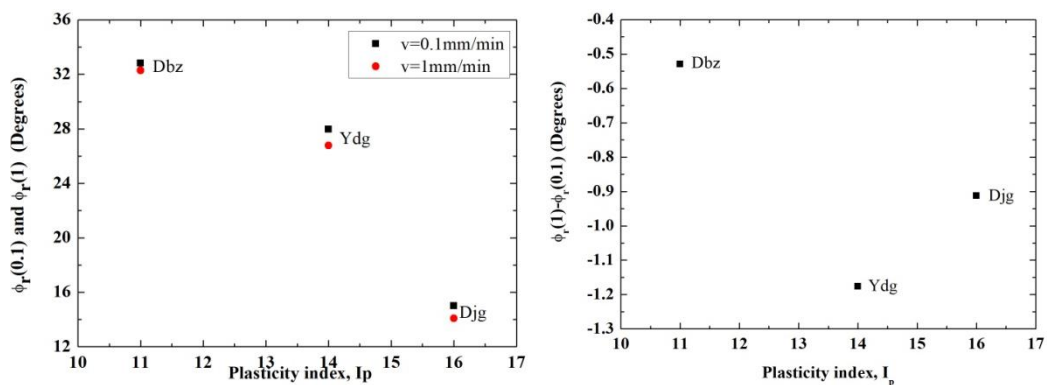
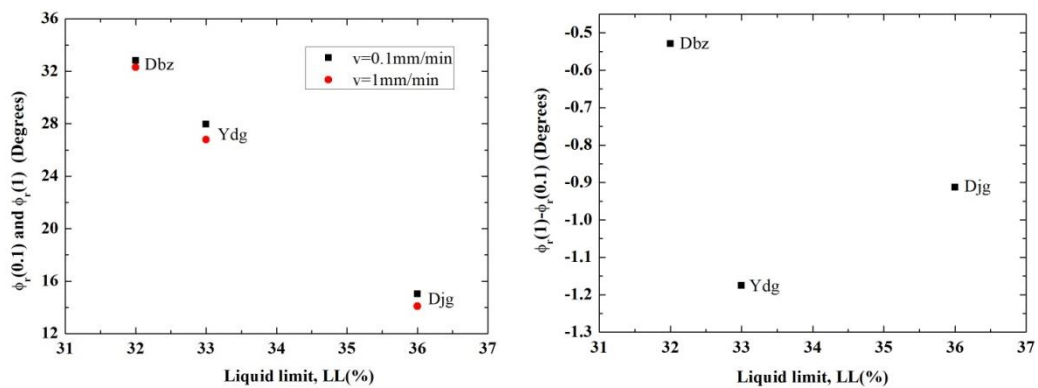
| No | Sample | Normal stress<br>(kN/m <sup>2</sup> ) | Residual strength parameter |                      |                        |                      | Difference in parameter                |                      |
|----|--------|---------------------------------------|-----------------------------|----------------------|------------------------|----------------------|--|----------------------|
|    |        |                                       | $\phi_{r(0.1)} (^\circ)$    |                      | $\phi_{r(1)} (^\circ)$ |                      | $\phi_{r(1)} - \phi_{r(0.1)} (^\circ)$ |                      |
|    |        |                                       | Under each $\sigma_n$       | Under all $\sigma_n$ | Under each $\sigma_n$  | Under all $\sigma_n$ | Under each $\sigma_n$                  | Under all $\sigma_n$ |
| 1  | Djg    | 100                                   | 16.699                      | 15.003               | 16.699                 | 14.090               | 0                                      | -0.913               |
|    |        | 200                                   | 15.563                      |                      | 15.642                 |                      | 0.079                                  |                      |
|    |        | 300                                   | 15.110                      |                      | 14.216                 |                      | -0.894                                 |                      |
|    |        | 400                                   | 14.708                      |                      | 13.496                 |                      | -1.212                                 |                      |
| 2  | Ydg    | 100                                   | 29.683                      | 27.954               | 27.474                 | 26.778               | -2.209                                 | -1.176               |
|    |        | 200                                   | 29.466                      |                      | 27.248                 |                      | -2.218                                 |                      |
|    |        | 300                                   | 27.923                      |                      | 26.870                 |                      | -1.053                                 |                      |
|    |        | 400                                   | 27.474                      |                      | 26.565                 |                      | -0.909                                 |                      |
| 3  | Dbz    | 100                                   | 38.660                      | 32.822               | 37.235                 | 32.293               | -1.425                                 | -0.529               |
|    |        | 200                                   | 34.019                      |                      | 33.425                 |                      | -0.594                                 |                      |
|    |        | 300                                   | 33.024                      |                      | 32.619                 |                      | -0.405                                 |                      |
|    |        | 400                                   | 32.005                      |                      | 31.487                 |                      | -0.518                                 |                      |

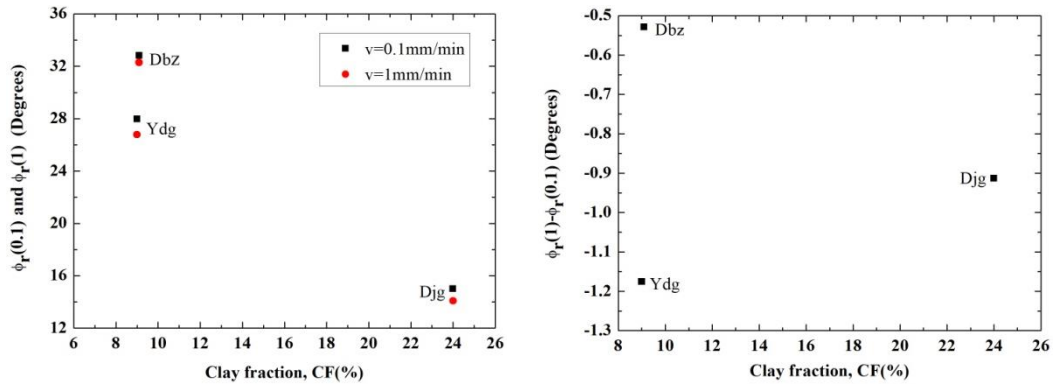
456

457 **4.4. Influence of the shear rate on the residual friction angles according to soil**  
 458 **properties**

459 It has been recognized that residual shear strength of soils is closely related with  
 460 soil properties, such as particle size distribution (PSD), liquid limit (LL), plasticity  
 461 index (Ip) and clay fraction (CF) (Terzaghi et al., 1996; Sayyah et al., 2016; Xu et al.,  
 462 2018; Eid et al., 2016). Fig. 11 depicts the relationships between residual friction  
 463 angles as well as the difference in the residual friction angles and soil properties  
 464 including LL, plasticity index (Ip) and clay fraction (CF) at two shear rates. The  
 465 residual friction angles at two shear rates decreased nonlinearly with the increasing of

466 the LL. As for the relationship between the  $\phi_r$  and  $I_p$ , the  $\phi_r$  under the low and high  
 467 shear rates decreases from about 32° to 15° with increasing the  $I_p$  from 11 to 16. These  
 468 findings agree well with the early studies (Wesley, 2003;Tiwari et al., 2005). With  
 469 increasing of CF from 9% to 24%, the residual friction angles under low and high  
 470 shear rates were found to decrease (Fig. 11). These observations are consistent with  
 471 previous studies (Lupini et al., 1981;Gibo et al., 1987). Interestingly, for Dbz and Ydg  
 472 soils of which have similar percentage of clay fraction, the residual friction angles at  
 473 both shear rates varied. However, in the relationships between the difference in the  
 474 residual friction angles and the soil properties, no clear correlations were found.





479

480

Fig. 11. Relationships between residual shear parameter, the difference in residual shear parameter and the soil properties at two shear rates

481

482

## 483 5. Conclusion

484

A series of ring shear tests were conducted on loess obtained from three landslides to study the residual shear characteristics of saturated loess. Based on the test results, the effect of the shear rate on the residual shear characteristics of loess in naturally drained condition was examined. The following conclusions can be drawn:

487

488

1. Ring shear test revealed that: (i) shear displacement to achieve the residual stage with high shear rate is greater than that of the low shear rate; (ii) Both the peak and residual friction coefficient became smaller with increase of shear rate for each sample; (iii) The greater difference between the peak and the residual friction coefficient in loess samples could be attributed to relatively well-developed slickenside on the shear surface.

489

490

491

492

493

494

2. At the two shear rates, there was a nonlinearly decrease trend of the residual friction coefficient with the normal stress in all loess samples. The difference between the friction coefficients,  $\tau_r/\sigma_n(1) - \tau_r/\sigma_n(0.1)$  was found to decrease

495

496

497

with normal stress in Ydg and Dbz specimens while increase with normal stress

498 in Djg specimens, indicating that CF may be closely associated with shear rate  
499 effect on residual friction coefficient with normal stress. Therefore, as for Ydg  
500 and Dbz with relatively low fraction of CF, there is an increase effect of shear  
501 rate on residual friction coefficient with decreasing of normal stress. Thus, for the  
502 application of measured residual friction coefficient for stability analysis of  
503 shallow landslides with lower overburden pressure, it is significant for us to use a  
504 low shear rate in ring shear tests to measure residual shear strength parameters.  
505 On other hand, for Djg with high CF, it is more reliable to use a low shear rate in  
506 ring shear tests to determine residual friction coefficient for stability analysis of  
507 deep landslides with high overburden pressure.

508 3. The difference at the two shear rates,  $\phi_r(1) - \phi_r(0.1)$ , under each normal stress  
509 level were either negative or positive. However, under all normal stress, the  
510 difference at the two shear rates  $\phi_r(1) - \phi_r(0.1)$  was found to be negative. Such  
511 negative shear rate effect on loess could be attributed to greater ability of clay  
512 particles in specimen to restore broken bonds at low shear rates.

513 4. The relationships between the  $\phi_r$  under two shear rates and soil properties (LL, Ip),  
514 demonstrated that the  $\phi_r$  at both shear rates decreased gradually with the  
515 increasing of LL and Ip. However, no clear correlations between the difference in  
516 the  $\phi_r$  at low and high shear rates and the soil properties were found.

517 A first attempt was made in this work to describe some shear rate effect on the  
518 residual characteristics of the saturated loess. The obtained experimental results do  
519 suggest that the residual shear behavior of saturated loess, can be affected, to a certain

520 extent, by the shear rate. However, a more quantitative evaluation of such effects, and  
521 a deeper understanding on the underlying processes must be achieved in order to  
522 assess their role in the initiation and mobility of loess landslides.

523

524

525 **Code availability:** Code can be made available by the authors upon request.

526 **Data availability:** Data can be made available by the authors upon request.

527 **Author contributions:** BL, XW, JP and QH conceived and designed the method; BL  
528 produced the results, and wrote the original manuscript under the supervision of XW  
529 and JP. JP and QH writing-review and editing.

530 **Competing interest:** The authors declare that they have no conflicts of interest.

531 **Acknowledgments:** This research was supported by the Major Program of National  
532 Natural Science Foundation of China (Grant No. 41790440), the National Natural  
533 Science Foundation of China (No.41902268) and the China Postdoctoral Science  
534 Foundation (No. 2019T120871). We thank Editor Professor Parise and anonymous  
535 reviewers for their constructive comments which help us improve the quality of the  
536 manuscript.

537 **References**

- 538 Ajmera, B., Tiwari, B., and Shrestha, D.: Effect of mineral composition and shearing rates on the  
539 undrained shear strength of expansive clays, in: *GeoCongress 2012: State of the Art and Practice in*  
540 *Geotechnical Engineering*, 1185-1194, 2012.
- 541 Bhat, D. R.: Effect of shearing rate on residual strength of kaolin clay, PhD, Graduate school of Science  
542 and Engineering, Ehime University, Japan, 2013.
- 543 Bishop, A. W., Green, G. E., Garga, V. K., Andresen, A., and Brown, J. D.: A new ring shear apparatus  
544 and its application to the measurement of residual strength, *Geotechnique*, 21, 273-328, 1971.
- 545 Bromhead, E.: *The stability of slopes*, blackie academic and professional, London. UK, 1992.
- 546 Chen, X., and Liu, D.: Residual strength of slip zone soils, *Landslides*, 11, 305-314, 2013.
- 547 Dijkstra, T., Rogers, C., Smalley, I., Derbyshire, E., Li, Y. J., and Meng, X. M.: The loess of north-central  
548 China: geotechnical properties and their relation to slope stability, *Engineering Geology*, 36, 153-171,  
549 1994.
- 550 Ding, H.: Ring shear tests on strength properties of loess in different regions. (In Chinese), Master,  
551 Northwest A&F University, 2016.
- 552 Eid, H. T.: Stability charts for uniform slopes in soils with nonlinear failure envelopes, *Engineering*  
553 *Geology*, 168, 38-45, 2014.
- 554 Eid, H. T., Rabie, K. H., and Wijewickreme, D.: Drained residual shear strength at effective normal  
555 stresses relevant to soil slope stability analyses, *Engineering Geology*, 204, 94-107, 2016.
- 556 Eid, H. T., Al-Nohmi, N. M., Wijewickreme, D., and Amarasinghe, R. S.: Drained Peak and Residual  
557 Interface Shear Strengths of Fine-Grained Soils for Pipeline Geotechnics, *Journal of Geotechnical and*  
558 *Geoenvironmental Engineering*, 145, 2019.
- 559 Fan, X., Xu, Q., Scaringi, G., Li, S., and Peng, D.: A chemo-mechanical insight into the failure mechanism  
560 of frequently occurred landslides in the Loess Plateau, Gansu Province, China, *Engineering Geology*,  
561 228, 337-345, 2017.
- 562 Gibo, S., Gashira, K., and Ohtsubo, M.: Residual strength of smectite-dominated soils from the  
563 Kamenose landslide in Japan, *Can Geotech J*, 24, 456-462, 1987.
- 564 Gratchev Ivan, B., and Sassa, K.: Shear strength of clay at different shear rates, *Journal of Geotechnical*  
565 *and Geoenvironmental Engineering*, 141, 2015.
- 566 Grelle, G., and Guadagno, F. M.: Shear mechanisms and viscoplastic effects during impulsive shearing,  
567 *Géotechnique* 41, 91-103, 2010.
- 568 Habibbeygi, F., and Nikraz, H.: Effect of shear rate on the residual shear strength of pre-sheared clays,  
569 *Cogent Geoscience*, 4, 1-9, 2018.
- 570 Hu, S., Qiu, H., Wang, X., Gao, Y., Wang, N., Wu, J., Yang, D., and Cao, M.: Acquiring high-resolution  
571 topography and performing spatial analysis of loess landslides by using low-cost UAVs. *Landslides*, 15,  
572 593-612, 2018.
- 573 Kimura, S., Nakamura, S., Vithana, S. B., and Sakai, K.: Shearing rate effect on residual strength of  
574 landslide soils in the slow rate range, *Landslides*, 11, 969-979, 10.1007/s10346-013-0457-6, 2014.
- 575 Kimura, S., Nakamura, S., and Vithana, S. B.: Influence of effective normal stress in the measurement  
576 of fully softened strength in different origin landslide soils, *Soil Till Res*, 145, 47-54, 2015.
- 577 Kramer, S., Wang, C., and Byers, M.: Experimental measurement of the residual strength of particulate  
578 materials, *Physics and mechanics of soil liquefaction*, 249-260, 1999.
- 579 Lemos, L.: Earthquake loading of shear surfaces in slopes, *Proc.11th I.C.S.M.F.E.*, 4, 1955-1958, 1985.

580 Leng, Y., Peng, J., Wang, Q., Meng, Z., and Huang, W.: A fluidized landslide occurred in the Loess  
581 Plateau: A study on loess landslide in South Jingyang tableland, *Engineering Geology*, 236, 129-136,  
582 2018.

583 Li, D., Yin, K., Glade, T., and Leo, C.: Effect of over-consolidation and shear rate on the residual strength  
584 of soils of silty sand in the Three Gorges Reservoir, *Scientific reports*, 7, 1-11, 2017.

585 Li, Y. R., Wen, B. P., Aydin, A., and Ju, N. P.: Ring shear tests on slip zone soils of three giant landslides in  
586 the Three Gorges Project area, *Engineering Geology*, 154, 106-115, 2013.

587 Lupini, J. F., Skinner, A. E., and Vaughan, P. R.: The drained residual strength of cohesive soils,  
588 *Geotechnique*, 31, 181-213, 1981.

589 Ma, P., Peng, J., Wang, Q., Zhuang, J., and Zhang, F.: The mechanisms of a loess landslide triggered by  
590 diversion-based irrigation: a case study of the South Jingyang Platform, China, *Bulletin of Engineering*  
591 *Geology and the Environment*, 78, 4945-4963, 2019.

592 Mesri, G., and Shahien, M.: Residual shear strength mobilized in first-time slope failures, *Journal of*  
593 *Geotechnical and Geoenvironmental Engineering*, 129, 12-31, 2003.

594 Moeyersons, J., Van Den Eeckhaut, M., Nyssen, J., Gebreyohannes, T., Van de Wauw, J., Hofmeister, J.,  
595 Poesen, J., Deckers, J., and Mitiku, H.: Mass movement mapping for geomorphological understanding  
596 and sustainable development: Tigray, Ethiopia, *Catena*, 75, 45-54, 2008.

597 Morgenstern, N. R., and Hungr, O.: High Velocity ring shear tests on sand, *Geotechnique*, 34, 415-421,  
598 1984.

599 Nakamura, S., Gibo, S., Egashira, K., and Kimura, S.: Platy layer silicate minerals for controlling residual  
600 strength in landslide soils of different origins and geology, *Geology*, 38, 743-746, 2010.

601 Okada, Y., Sassa, K., and Fukuoka, H.: Excess pore pressure and grain crushing of sands by means of  
602 undrained and naturally drained ring-shear tests, *Engineering Geology*, 75, 325-343, 2004.

603 Osipov, V., Nikolaeva, S., and Sokolov, V.: Microstructural changes associated with thixotropic  
604 phenomena in clay soils, *Geotechnique*, 34, 293-303, 1984.

605 Pakbaz, M., Behzadipour, H., and Ghezlbash, G.: Evaluation of shear strength parameters of sandy  
606 soils upon microbial treatment, *Geomicrobiology journal*, 35, 721-726, 2018.

607 Perret, D., Locat, J., and Martignoni, P.: Thixotropic behavior during shear of a fine-grained mud from  
608 Eastern Canada, *Engineering Geology*, 43, 31-44, 1996.

609 Picarelli, L.: Discussion on "A rapid loess flowslide triggered by irrigation in China" by D. Zhang, G.  
610 Wang, C. Luo, J. Chen, and Y. Zhou, *Landslides*, 7, 203-205, 2010.

611 Sassa, K., Fukuoka, H., Wang, G., and Ishikawa, N.: Undrained dynamic-loading ring-shear apparatus  
612 and its application to landslide dynamics, *Landslides*, 1, 7-19, 2004.

613 Sayyah, A., Eriksen, R. S., Horenstein, M. N., and Mazumder, M. K.: Performance analysis of  
614 electrodynamic screens based on residual particle size distribution, *IEEE Journal of Photovoltaics*, 7,  
615 221-229, 2016.

616 She, X.: The formation mechanism of landslide of loess and bedrock contact surface (in Chinese),  
617 Master, Chang'an China, 2015.

618 Shinohara, K., and Golman, B.: Dynamic shear properties of particle mixture by rotational shear test,  
619 *Powder Technol*, 122, 255-258, 2002.

620 Skempton, A. W.: Long-term stability of clay slopes, *Geotechnique*, 14, 77-102, 1964.

621 Skempton, A. W.: Residual strength of clays in landslides, folded strata and the laboratory,  
622 *Geotechnique*, 35, 3-18, 1985.

623 Skempton: Long-term stability of clay slopes, *Geotechnique*, 14, 77-102, 1964.



624 Stark, T. D., and Vettel, J. J.: Bromhead ring shear test procedure, *Geotech Test J*, 15, 24-32, 1992.

625 Stark, T. D., Choi, H., and McCone, S.: Drained shear strength parameters for analysis of landslides,  
626 *Journal of Geotechnical and Geoenvironmental Engineering*, 131, 575-588, 2005.

627 Stark Timothy, D., Choi, H., and McCone, S.: Drained shear strength parameters for analysis of  
628 landslides, *Journal of Geotechnical and Geoenvironmental Engineering*, 131, 575-588, 2005.

629 Summa, V., Tateo, F., Giannossi, M., and Bonelli, C.: Influence of clay mineralogy on the stability of a  
630 landslide in Plio-Pleistocene clay sediments near Grassano (Southern Italy), *Catena*, 80, 75-85, 2010.

631 Summa, V., Margiotta, S., Medici, L., and Tateo, F.: Compositional characterization of fine sediments  
632 and circulating waters of landslides in the southern Apennines–Italy, *Catena*, 171, 199-211, 2018.

633 Sun, P., Peng, J., Chen, L., Yin, Y., and Wu, S.: Weak tensile characteristics of loess in China — An  
634 important reason for ground fissures, *Engineering Geology*, 108, 153-159, 2009.

635 Suzuki, M., Tsuzuki, S., and Yamamoto, T.: Residual strength characteristics of naturally and artificially  
636 cemented clays in reversal direct box shear test, *Soils And Foundations*, 47, 1029-1044, 2007.

637 Terzaghi, K.: *Theoretical soil mechanics*, Chapman And Hall, Limited.; London, 1951.

638 Terzaghi, K., Peck, R. B., and Mesri, G.: *Soil mechanics in engineering practice*, John Wiley & Sons,  
639 1996.

640 Tika, T.: Ring shear tests on a carbonate sandy silt, *Geotechnical Testing Journal*, 22, 1999.

641 Tika, T. E., Vaughan, P. R., and Lemos, L. J. L. J.: Fast shearing of pre-existing shear zones in soil,  
642 *Geotechnique*, 46, 197-233, 1996.

643 Tika, T. E., and Hutchinson, J. N.: Ring shear tests on soil from the Vaiont landslide slip surface,  
644 *Geotechnique*, 49, 59-74, 1999.

645 Tiwari, B.: *Analysis of landslide mechanism of Okimi Landslide*, M. Sc. Thesis, Niigata University, 2000.

646 Tiwari, B., Brandon, T. L., Marui, H., and Tuladhar, G. R.: Comparison of residual shear strengths from  
647 back analysis and ring shear tests on undisturbed and remolded specimens, *Journal of Geotechnical  
648 and Geoenvironmental Engineering*, 131, 1071-1079, 2005.

649 Tiwari, B., and Marui, H.: A new method for the correlation of residual shear strength of the soil with  
650 mineralogical composition, *Journal of Geotechnical and Geoenvironmental Engineering*, 131,  
651 1139-1150, 2005.

652 Tiwari, G., and Latha, G. M.: Reliability analysis of jointed rock slope considering uncertainty in peak  
653 and residual strength parameters, *Bulletin of Engineering Geology and the Environment*, 78, 913-930,  
654 2019.

655 Vithana, S. B., Nakamura, S., Kimura, S., and Gibo, S.: Effects of overconsolidation ratios on the shear  
656 strength of remoulded slip surface soils in ring shear, *Engineering Geology*, 131-132, 29-36, 2012.

657 Wang, J., Li, P., Ma, Y., and Vanapalli, S. K.: Evolution of pore-size distribution of intact loess and  
658 remolded loess due to consolidation, *Journal of Soils and Sediments*, 19, 1226-1238, 2019.

659 Wang, S., Wu, W., Xiang, W., and Liu, Q.: Shear behaviors of saturated loess in naturally drained  
660 ring-shear tests, in: *Recent Advances in Modeling Landslides and Debris Flows*, Springer, 19-27, 2015.

661 Wang, W.: *Residual Strength of Remolded Loess in Ring Shear Tests.*, PhD Northwest A & F University  
662 of China, 2014.

663 Wesley, L.: Stability of slopes in residual soils, *Obras y Proyectos*, 47-61, 2018.

664 Wesley, L. D.: Residual strength of clays and correlations using atterberg limits, *Geotechnique*, 23,  
665 669-672, 2003.

666 Xu, C., Wang, X., Lu, X., Dai, F., and Jiao, S.: Experimental study of residual strength and the index of  
667 shear strength characteristics of clay soil, *Engineering Geology*, 233, 183-190, 2018.

668 Yan, G., Qi, F., Wei, L., Aigang, L., Yu, W., Jing, Y., Aifang, C., Yamin, W., Yubo, S., and Li, L.: Changes of  
669 daily climate extremes in Loess Plateau during 1960–2013, *Quaternary international*, 371, 5-21, 2015.  
670 Zhang, D., Wang, G., Luo, C., Chen, J., and Zhou, Y.: A rapid loess flowslide triggered by irrigation in  
671 China, *Landslides*, 6, 55-60, 2009.  
672 Zhang, M., Jiao, P., and Wei, X.: Study on development characteristics and distribution regularity of  
673 landslide and geohazards in baota district, yan'an (in Chinese), *Hydrogeology and Engineering Geology*,  
674 33, 72-74, 2006.  
675